Vibrational and rotational population distributions of MgH($v''=0$ and 1) produced in the reaction of Mg($3s3p\ ^1P_1$) with H_2

Dean-Kuo Liu, Thou-Long Chin, and King-Chuen Lin*
Department of Chemistry, National Taiwan University and Institute of Atomic and Molecular Sciences, Academia Sinica, Taipei, Taiwan 10764, Republic of China
(Received 5 April 1994)

The population distributions of the rotational quantum states of the nascent MgH($v''=0$ and 1) produced in the reaction of Mg($3s3p\ ^1P_1$) with H_2 are bimodal. With the use of the surprisal method, the two components are separated. The minor low-N component of the distribution in the $v''=0$ state is found to be larger than that in the $v''=1$ state, whereas, the major high-N component of the distribution in the $v''=0$ state becomes roughly equivalent to that in the $v''=1$ state. The two parallel low-N and high-N processes are expected to correspond to two distinct types of reaction dynamics. One (minor) type produces MgH in lower rotational levels and preferentially $v''=0$, and the other (major) type produces MgH in higher rotational levels with comparable $v''=0$ and $v''=1$ populations. Possible dynamical models are discussed.

PACS number(s): 82.30.−b, 34.50.−s, 35.20.−i

I. INTRODUCTION

By using a pump-and-probe method in the study of the reaction

$$Mg(3s3p\ ^1P_1)+H_2\rightarrow MgH(v'',N)+H\ , \quad (1)$$

Breckenridge and Umemoto have demonstrated that the rotational population distribution of the nascent product MgH($v''=0$) was characterized by a bimodality [1]. Two parallel reaction mechanisms of insertion and abstraction were proposed previously. The large component over the higher rotational quantum states was considered previously to follow a mechanism of Mg insertion into the H_2 bond by a side-on attack, thus leading to a bent intermediate MgH_2 state. As one terminal H atom escapes, a rotational torque is exerted upon the remaining MgH, leading to population distribution in the higher rotational quantum states. In contrast, a small portion of lower rotational energy distribution was proposed to proceed with a reactive approach having a collinear configuration. Thus the mechanism of H abstraction by the end-on attack may not impact on the rotational energy of MgH significantly [1]. In a recent investigation, probing the transient intermediate MgH_2 with use of matrix isolation method at 12 K, McCaffery *et al.* have identified the linear structure H—Mg—H to be the only stable configuration [2]. They also safely ruled out the possibility of "cage effect," which may facilitate the recombination of MgH and H, the fragments resulting from the H-abstraction pathway. This fact suggests that MgH+H product in the gas-phase reaction should result from the reactive approach of Mg insertion. In addition, through the experiments of isotopic effect [3] and temperature dependence measurement [4], more evidences are provided to shed light on the understanding of the mechanisms leading to the bimodal nature.

Breckenridge and Wang, using isotopic hydrogens as reagents, showed a profile coincidence of rotational state distribution of MgH($v''=0$) produced either from HD or H_2 [3]. The lack of a significant isotopic effect suggested that the bimodality may originate from a single mechanism. They concluded that Eq. (1) is an exit-channel controlled reaction, which is dominated by the insertive mechanism. From the calculation of dynamical-potential-energy surfaces, the reaction coordinate for the insertive mechanism, which leads to a bent intermediate state (C_{2v}) of MgH_2, tracks an attractive $^1B_2$ surface without suffering from an activation barrier. On the contrary, for a collinear approach of Mg($^1P_1$) toward H_2, there exists a barrier as large as 1.8 or 1.7 eV as either a $^1\Sigma^+$ or a $^1\Pi$ surface is followed, respectively [5]. Since the energy barrier differs for MgH produced through collinear and bent colliding geometries, these two reaction mechanisms should have a different temperature dependence. In our previous experiments on the temperature dependence, the rotational population distributions of the nascent MgH product obtained at various temperatures were coincident with each other [4]. This suggests that the bimodal nature originates from a single insertive mechanism.

Although a profound insight into the reaction (1) has thus been gained, the detailed pathways leading to the rotational bimodality are still questionable. It is believed that this reaction is exit-channel controlled, forming the MgH product through two distinct pathways; one corresponds to the high-N component of the rotational state distribution, and the other is relevant with the low-N state distribution. From the theoretical point of view, Chaquin, Sevin, and Yu have suggested that the electronic state $^1B_2-^3A_1$ surface crossing may explain the formation of the small low-N component of the distribution [5]. The $^3A_1$ surface correlates with the ground electronic

*Author to whom correspondence should be addressed.

state of linear structure Mg—H—H, from which the terminal H atom escapes without causing significant rotational excitation of MgH. Breckenridge and Umemoto found the vibrational population decreased with increasing v'' [1]. Accordingly, they suggested that the rate of internal energy randomization of MgH_2 is as fast as that of decomposition of MgH_2, and the reaction also involves a very late release of potential energy.

In this paper we present more detailed information on the vibrational population distribution of MgH produced in the reaction (1). Although Breckenridge and Umemoto have reported the rotational population of MgH($v''=1$) as determined by computer simulation [1], the way they extracted the spectrum information turns out to be less reliable. In addition, they assumed the rotational state distribution of MgH($v''=1, N''=1-20$) to be relevant to an understanding of the proposed entrance-channel reaction pathway, which has been proven to be wrong in the latter experiments of isotope and temperature effects [3,4]. The rotational population distributions in both $v''=0$ and 1 states obtained herein appear to be bimodal; the two components contained may be deconvoluted with use of the linear surprisal method. The minor low-N component of the distribution in the $v''=0$ state is found to be larger than that in the $v''=1$ state, whereas the major high-N component of the distribution becomes roughly equivalent to that in the $v''=1$ state. Therefore, two parallel pathways are expected to be relevant with the reaction dynamics. One type produces MgH in low rotational levels and preferentially $v''=0$, and the other type produces MgH in higher rotational levels with comparable $v''=0$ and $v''=1$ populations. By using the *ab initio* calculation of dynamical-potential-energy surfaces obtained by Chaquin, Sevin, and Yu [5], we are able to satisfactorily interpret the deconvoluted ro-vibrational population distributions and suggest the possible mechanistic processes that lead to a feature of rotational bimodality in the subject reaction.

II. EXPERIMENT

The pump-and-probe technique used in this work has been illustrated previously [4,6] and described in detail elsewhere [1,7]. Briefly, the pump-and-probe technique employed two dye lasers which were pumped, respectively, by a frequency-doubled and a frequency-tripled 10 Hz, 5–8 ns neodymium-doped yttrium aluminum garnet (Nd:YAG) laser. The pump laser was operated with mixed dyes of rhodamine 590 and rhodamine 610. The tunable output near 570 nm was frequency doubled to 285 nm, which excited the Mg atomic vapor to the $3\,^1P_1$ state. The laser energy was low enough to ensure that a one-photon excitation process was involved. The resulting MgH product was monitored with laser-induced fluorescence (LIF) in the $A\,^2\Pi-X\,^2\Sigma^+$ bands using a probe laser with less than a 20 ns delay with respect to the pump laser. Given the H_2 pressure in the chamber in the range of 0.5–4 Torr, the delay time was adjusted so that the MgH observed was collision free. Both lasers propagated collinearly and their powers were monitored continuously with an individual photodiode. The energy of the unfocused pump beam was 100–400 μJ for Mg($^1P_1$) excitation, while the unfocused probe beam was about 100 μJ.

The obtained LIF signal of (0,0) and (0,1) bands [(v',v'') notation used] was focused by means of two lenses onto a monochromator. The center wavelength of the grating was set to 560 nm and 517 nm, respectively, for the $v'=0\rightarrow v''=1$ and $v'=0\rightarrow v''=0$ transitions. As the slits were 5 mm wide, the monochromator with dispersion 1.8 nm/mm acted as an interference filter having 9 nm bandpass. Thus the transmitted LIF signal was detected by an attached photomultiplier tube. To obtain a wide range of spectra, the slits were opened to 8 mm. The signal was processed by a boxcar integrator and then normalized to the condition of the identical power of laser irradiation. A microcomputer interfaced to the boxcar integrator stored the data for further treatment.

The reaction chamber was a stainless steel five-armed cross heat-pipe oven, allowing for spectral observation perpendicular to the laser axis [4,6,7]. A thermocouple, inserted through the top arm in the vicinity of the reactive region, was used to monitor the oven temperature with an accuracy ± 1 K. The Mg metal was deposited and heated to 750–760 K, corresponding to a vapor pressure of 40–50 mTorr. The pressure of gaseous H_2 in the oven was maintained from 0.5 to 4 Torr with an MKS Baratron manometer.

III. RESULTS AND DISCUSSION

A. Laser-induced fluorescence spectra of MgH

The LIF spectra of the (0,0) and (0,1) bands in the $A\,^2\Pi-X\,^2\Sigma^+$ transition of the nascent MgH product were obtained following excitation of Mg($^1P_1$) at 285.2 nm. The rotational lines of $N=1-10$ and 21–30 for the P branch in the (0,0) band, and those of $N=1-7$ and 15–27 in the (0,1) band can be resolved completely under our laser conditions with resolution ≤ 1 cm^{-1}. However, the $N=11-20$ lines of the (0,0) band and the $N=8-14$ lines of the (0,1) band overlap severely, so that a computer simulation is applied to obtain the deconvoluted spectra [4]. A satisfactory agreement between the simulated spectra and the LIF spectra of the (0,1) band is revealed in Fig. 1. Note that the Q and R branches in the (0,1) band have onsets close to the P branch with $N\geq 20$, and therefore they may interfere significantly with the high-N component of the P branch. With the Q and R branches taken into account in the simulation, fortunately several high-N rotational lines such as $P_1(21)$, $P_1(22)$, $P_1(24)$, $P_1(25)$, $P_1(26)$, and $P_2(27)$ may be resolved from the Q and R branches, and their intensities can be estimated within a small error. Because of the good spectral resolution, the P_1 branch is selected for determination of the rotational distribution.

For detecting the population in the $v''=0$ state, the (0,0) band is excited while the emission band of (0,1) is monitored. In contrast, for detecting the population in the $v''=1$ state, the (0,1) band is excited and then the (0,0) band is monitored. Although the Franck-Condon factor for the $v''=1\rightarrow v'=0$ excitation transition is about

an order of magnitude smaller than that of transition $v''=0\rightarrow v'=0$, the small transition probability is compensated by monitoring a strong emission band (0,0). Accordingly, while comparing the total population between the $v''=0$ and $v''=1$ states, there is no need to take into account the Franck-Condon factor for correction.

B. Analysis of rotational state distribution

In the electronic transition $A\,^2\Pi-X\,^2\Sigma^+$ of MgH, the ground state belongs to Hund's case (b), while the $A\,^2\Pi$ state is considered to be a case intermediate between (a) and (b). Hund's case (b) dominates with increasing N, causing spin-decoupling with the molecular axis. However, Hund's case (a) becomes important for those low-N rotational lines, depending upon the ratio of A/B_v, in which A denotes the coupling constant between the spin and the orbital angular momentum and B_v is the rotational constant [8]. The value of A/B_v is indicative of the strength of the spin coupling to the molecular axis. When the ratio approaches to zero, the transition type belongs to Hund's case (b), whereas it tends to be close to Hund's case (a) as the ratio approaches to $\pm\infty$. For the case of MgH, the values of A and B_v are 35.3 and 6.09 for $v''=0$, respectively, and thus the ratio equals 5.8. For such an intermediate case, the intensity of the four satellite transition lines ($^PQ_{12}$, $^RQ_{21}$, $^QR_{12}$, and $^QP_{21}$) are not negligible, especially in the low-N region. The only satellite branch that may disturb the assigned P_1 and P_2 lines is $^PQ_{12}$, of which the wavelength difference from the P_1 branch depends upon the spin splitting between the doublets of the $X\,^2\Sigma^+$ state. Because the spin-splitting constant is as small as 0.025 cm^{-1} [8], the satellite branch $^PQ_{12}$ occurs essentially at the same frequency as the P_1 branch under our laser conditions. According to the Hönl-London formula derived by Earls [9] and Breckenridge [10], the intensities of rotational lines of the P_1 branch are estimated to be 0.167, 0.391, 0.633, and 0.880, and 1.13 for $N=1,2,3,4$, and 5, respectively, while the intensities of the $^PQ_{12}$ satellite branch are estimated to be 0.333, 0.205, 0.149, 0.115, and 0.093. The ratio of $P_1(N)/^PQ_{12}(N)$ increases rapidly with increasing quantum number N, and therefore the observed intensities of the P_1 lines that may be masked significantly by the satellite branch are limited within a few low-N states.

By taking into account the Hönl-London factor and intensity correction with subtraction of the satellite $^PQ_{12}$ from the observed P_1 branch, the rotational state distributions of MgH in the $v''=0$ and 1 states appear to be bimodal. As shown in Figs. 2 and 3, both population distri-

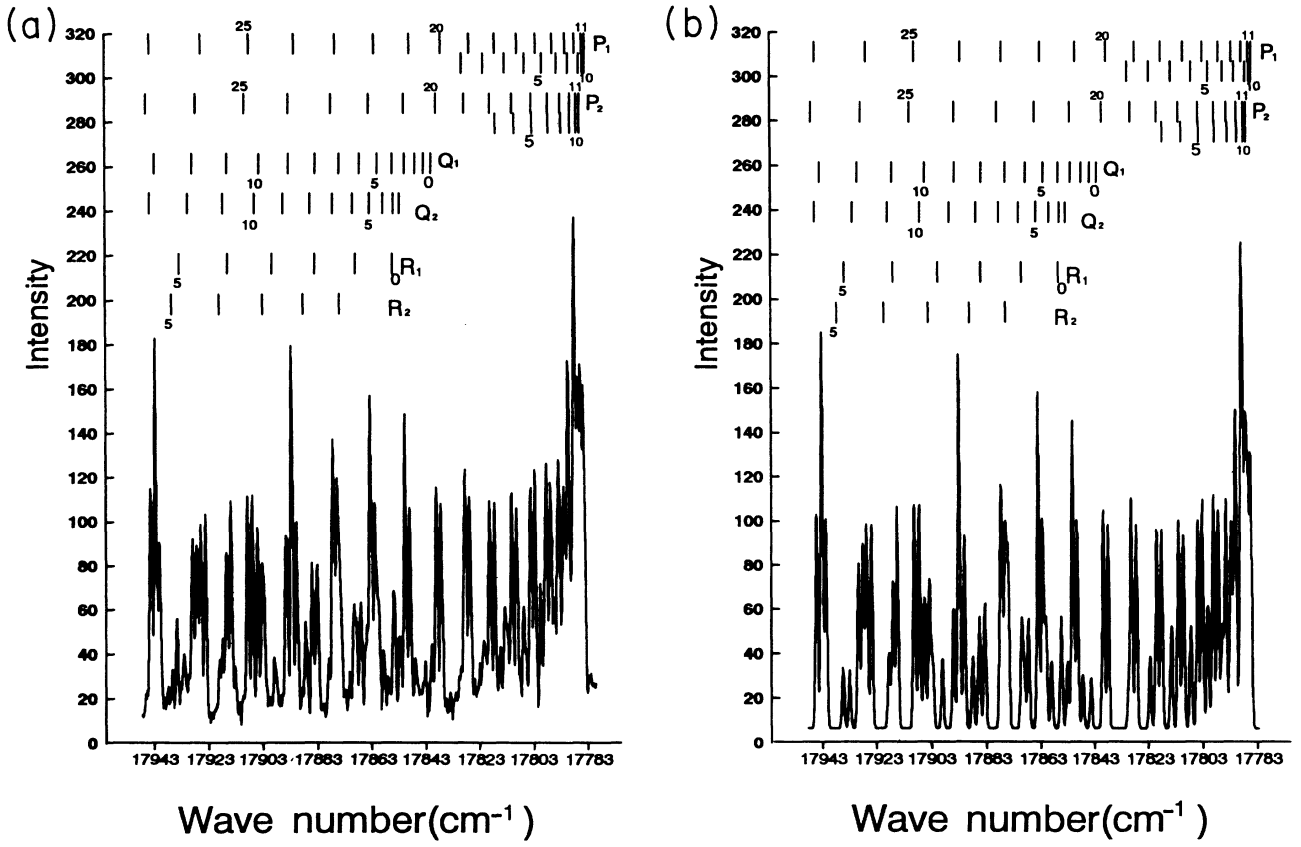

FIG. 1. (a) A portion of LIF spectra for the P, Q, and R branches in the (0,1) band of the MgH ($A\,^2\Pi-X\,^2\Sigma^+$) transition. (b) Spectra by computer simulation of the same region. MgH($v''=1$) is a nascent product in the reaction of Mg($^1P_1$) with H_2. Computer-simulated spectra can best fit the experimental result.

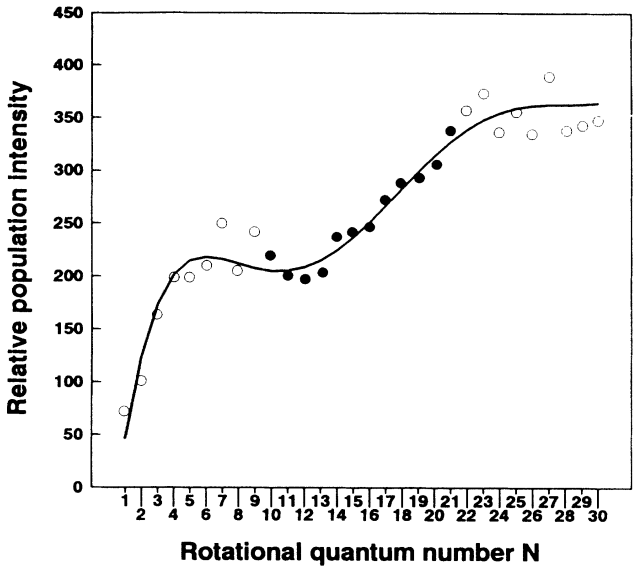

FIG. 2. Rotational population distribution of MgH in the $v''=0$ state. The open circles denote the experimental finding of the P_1 branch; the closed circles denote the deconvoluted spectra around the bandhead by computer simulation. The solid line is the least-squares fit based on a sixth power polynomial.

butions are represented by the P_1 branch, which turns out to be less overlapped spectrally in the high-N component especially for the (0,1) band. The rotational population distribution in the $v''=0$ state, represented by the P_1 branch, is consistent with those reported by Breckenridge and co-workers [1,3] and our previous work [4] using the average of the P_1 and P_2 branches instead. For

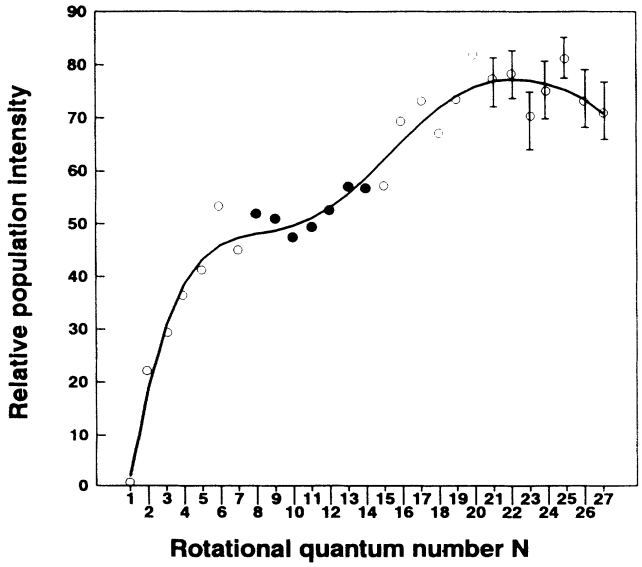

FIG. 3. Rotational population distribution of MgH in the $v''=1$ state. The open circles denote the experimental finding of the P_1 branch; the closed circles denote the deconvoluted spectra around the bandhead by computer simulation. The solid line is the least-squares fit based on a sixth-power polynomial.

the $v''=0$ state, the peak ratio of the large-N component to the small-N component gives a value of ~ 1.7, in agreement with those reported [1,4]. As shown in Figs. 2 and 3, the intensity of bimodal distribution in the $v''=1$ state is essentially as large as that in the $v''=0$ state. By summing up the population intensity of each rotational line, our measurement of population ratio of MgH($v''=1$) to MgH($v''=0$) reaches 0.8 ± 0.1, in agreement with the value of 0.7 ± 0.2 obtained by Breckenridge and Umemoto [1].

C. Comparison of methods used to analyze $v''=1$ population distribution

Breckenridge and Umemoto measured the rotational state distribution of MgH($v''=1$) following excitation of the (1,1) band and monitoring emission of the (1,0) band [1]. Their treatment by computer simulation to find the MgH($v''=1$) population distribution is less reliable, despite the fact that their determined population ratio of MgH($v''=1$) to MgH($v''=0$) is consistent with ours [1]. The excitation spectrum of the (1,1) band is severely blended by the P_1, P_2, Q_1, Q_2, R_1, and R_2 branches of the (0,0) band. It is insensitive and less reliable to extract information on the $v''=1$ population from such a congested spectrum. To examine the sensitivity of such a simulation method, we have simulated the (0,0) band, presuming that Q and R doublets have the identical trend of the population distribution as the P branch found in this work. Let us compare two simulated spectra; one consists of P, Q, and R branches in the $v''=0$ state with identical trend of population distribution, and the other contains P, Q, and R branches but the population intensities of the Q and R branches are reduced purposely by a factor of two. As one can see in Fig. 4, it is somehow difficult to tell a significant difference between them. Note that the (1,1) band is omitted in the figures, and its onset is indicated by an arrow. The (1,1) band is apparently buried in a very nasty environment. Thus, using the (1,1) band to extract information on the $v''=1$ state should be less reliable. In contrast, the rotational spectrum of MgH in the (0,1) band is well resolved up to $N=27$ for the P branch except for the lines around the bandhead, of which the resolution relies upon the computer simulation. In addition, the small-N component has been corrected for its intensity by considering the contribution of satellite $^PQ_{12}$. The rotational population distribution in the $v''=1$ state obtained in this work is apparently more acceptable.

D. Surprisal analysis

With use of the linear surprisal method [11], the high-N component of the rotational population distribution of MgH($v''=0$ and 1) can be fitted satisfactorily, and thus the small, low-N component may be deconvoluted as shown in Fig. 5. As compared with the rotational population distribution of MgH($v''=0$), MgH($v''=1$) is found to have a comparable distribution for the high-N component, but a smaller distribution for the low-N com-

ponent. For a more quantitative comparison of the bimodality between MgH($v''=0$) and MgH($v''=1$), the total population intensity of each deconvoluted rotational profile is evaluated in Fig. 6. The population ratio of MgH($v''=1$) to MgH($v''=0$) for the low-N component gives a value of 0.42 ± 0.05, slightly smaller than that of 0.65 ± 0.10 obtained by Breckenridge and co-workers, whereas the population ratio of 0.87 ± 0.05 for the high-N component becomes larger than their result.

E. Mechanism for high-N component of rotational state distribution

With the aid of the vibrational population distribution, the puzzle of the reaction mechanisms causing the rotational bimodality of MgH produced in reaction (1), which was first proposed a decade ago, can be satisfactorily solved. As shown in Fig. 6, two parallel mechanistic processes are expected to be relevant with this bimodal feature. The major process causes the resulting MgH populated in the high rotational states, whereas the minor one leads to the low rotational states. It is feasible to interpret the mechanism leading to the high rotational population distribution.

In the calculation of dynamical potential energy surfaces, Chaquin, Sevin, and Yu [5] found that the side-on, Mg-insertive mechanism follows an attractive $^1B_2$ surface, while the head-on, H-abstractive mechanism must suffer from a large energy barrier. Through the measurements of isotopic effect [3] and temperature effect [4] upon the LIF spectra of MgH, it is believed that the bimodality results from a side-on, reactive approach of Mg—H_2 collision. The reaction pathway following the attractive $^1B_2$ surface crosses the $^1A'$ (or $^1A_1$) surface, which correlates with Mg+H_2 reactants and MgH+H products in C_s (or C_{2v}) geometry [5]. The $^1B_2$ surface cannot couple to the $^1A'$ (or $^1A_1$) surface in C_s (or C_{2v}) symmetry, unless the asymmetric stretch mode ($^1b_2$ symmetry) is excited. A schematic diagram describing the symmetry correlation and the relevant surface crossing is shown in Fig. 7(a). As Mg* approaches H_2 side-on, the bending mode of MgH_2 is expected to be excited. To form H ($^2S_{1/2}$)+MgH($X\,^2\Sigma^+$), the bending mode should couple with the asymmetric stretch mode. Accordingly, the energy transfer from the bending mode into the asym-

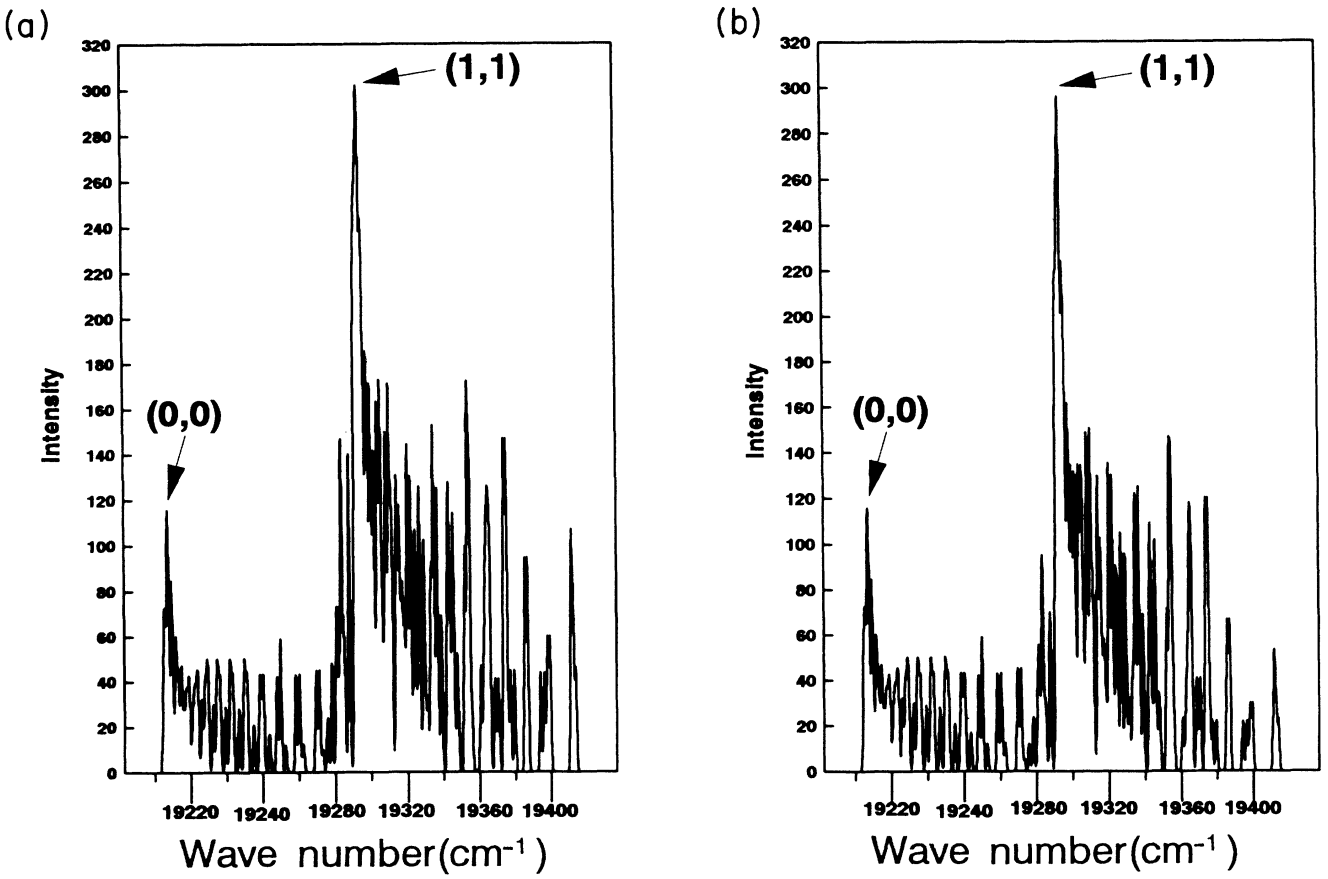

FIG. 4. (a) Simulated spectra of the P, Q, and R branches in the (0,0) band with identical trend of the population distribution as the P branch found in this work. The arrow indicates onset of the (1,1) band, which is omitted in the simulation. (b) Simulated spectra of the P, Q, and R branches in the (0,0) band with the population intensity of the Q and R branches reduced to a half purposely with respect to the P branch. The arrow indicates onset of the (1,1) band, which is omitted in the simulation.

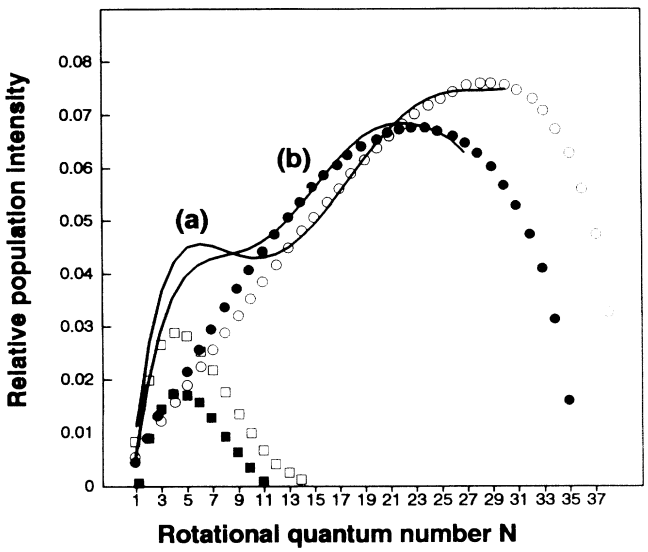

FIG. 5. Solid lines, (a) and (b) indicate the nascent rotational population distribution of MgH in the $v''=0$ and $v''=1$ states, respectively, as determined in Figs. 2 and 3. Closed circles, the high-N component of MgH($v''=1$) fitted using the linear surprisal method. Closed squares, the low-N component of MgH($v''=1$) deconvoluted from subtraction of solid line (b). Open circles, the high-N component of MgH($v''=0$) fitted using the linear surprisal method. Open squares, the low-N component of MgH($v''=0$) deconvoluted from subtraction of solid line (a).

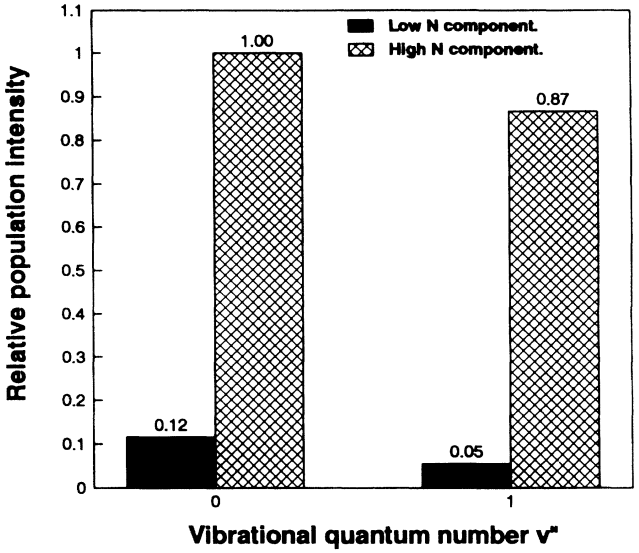

FIG. 6. Comparison of the relative vibrational population of MgH in the $v''=0$ and $v''=1$ states. The intensity is summed respectively over the rotational profiles of low-N and high-N components deconvoluted.

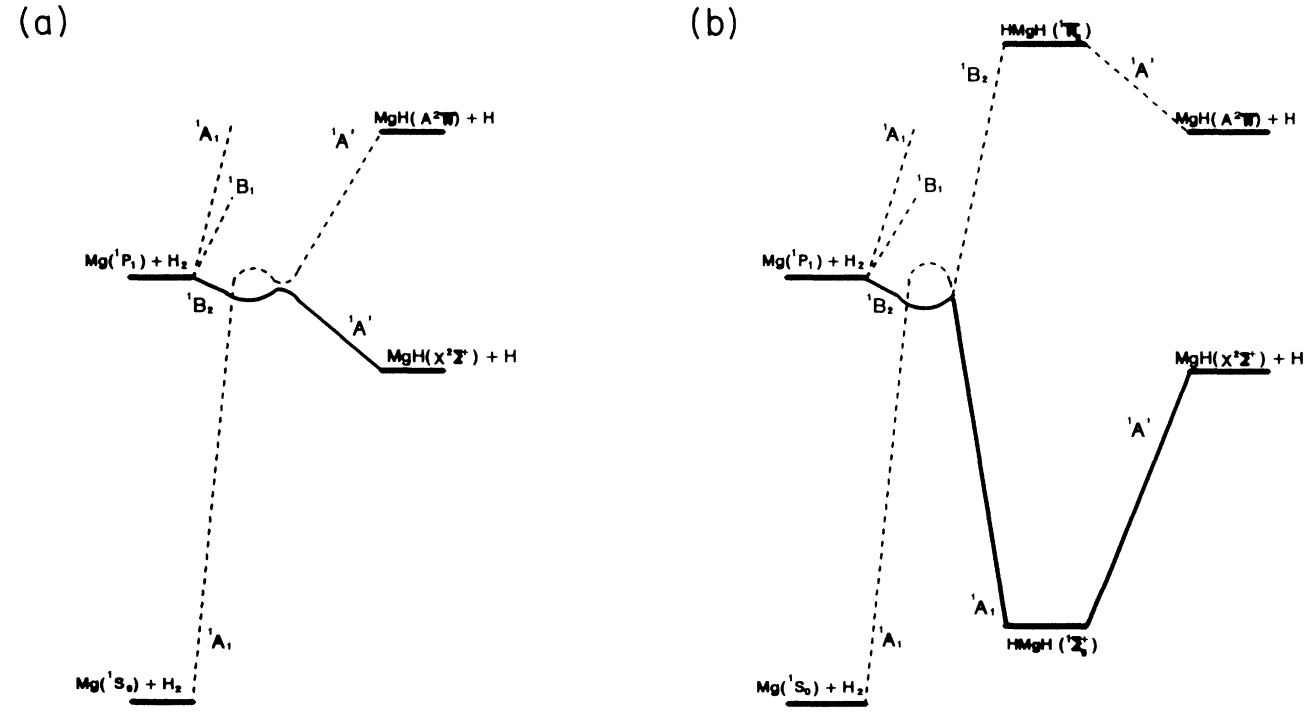

FIG. 7. (a) Symmetry correlation diagram for the reaction of Mg($^1P_1$) with H_2 in a C_{2v} collisional configuration. The energy of each state follows the data calculated by Chaquin, Sevin, and Yu. The barrier formed between the ground reactants Mg($^1S_0$)+H_2 and the products MgH($X^2\Sigma^+$)+H($^2S_{1/2}$) in a C_{2v} configuration is also based on their result. (b) Symmetry correlation diagram for the reaction of Mg($^1P_1$) with H_2 in a C_{2v} collisional configuration, in which the long-lived, linear intermediate HMgH is involved. The energy of each state follows the data calculated by Chaquin, Sevin, and Yu. The barrier formed between the ground reactants Mg($^1S_0$)+H_2 and the intermediate HMgH is also based on their result.

metric stretch mode may facilitate the release of H atom and also cause an effective vibrational motion of the remaining MgH. In addition, a torque is exerted upon the MgH to cause population in the high rotational states. This interpretation is consistent with our observation that the high-N component of rotational state distribution is accompanied by a hot vibrational state distribution. In terms of the *ab initio* calculation of dynamical potential energy surfaces from Chaquin, Sevin, and Yu and the ro-vibrational state distribution, we are able to interpret satisfactorily the mechanistic process that leads to the high-N component of rotational state distribution.

F. Mechanism for low-N component of rotational state distribution

Concerning the formation of the low-N component of the rotational state distribution, the mechanisms proposed are rather ambiguous [1,5]. Chaquin, Sevin, and Yu suggest that the reaction coordinate along the $^1B_2$ surface may cross the $^3A_1$ surface, which correlates with the linear configuration of Mg—H—H [5]. If such a singlet-to-triplet surface crossing does happen, the kinetic energy along the MgH molecular axis may not impact upon the rotational states significantly, as the other H atom departs. Moreover, for the *HLL* (H=heavy atom, L=light atom) linear structure, the kinematic effect caused by escape of the end H atom may lead to a significant vibrational motion of MgH. The resulting MgH should be vibrationally hot, but rotationally cold. This interpretation is apparently against our experimental findings of MgH which is populated in low-N state distribution and preferentially $v''=0$.

A plausible alternative pathway leading to the low-N state distribution of MgH is suggested as follows. In the *ab initio* calculation of the potential energy surface, the reaction coordinate along the $^1B_2$ surface crosses the $^1A_1$ state, which correlates with the ground electronic states of the $Mg(^1S_0)+H_2(^1\Sigma_g^+)$ reactants and the linear intermediate HMgH in C_{2v} symmetry. The correlation diagram is depicted in Fig. 7(b). The state energy follows the data calculated by Chaquin, Sevin, and Yu [5]. The bending mode of HMgH, in which the kinetic energy is initially deposited, may couple efficiently with the asymmetric stretch mode $^1b_2$ to induce a vibronic transition between the surfaces of $^1B_2$ and $^1A_1$. As one H atom departs from the *LHL* linear structure, the kinematic effect acts insignificantly on the remaining MgH, so that the MgH product stays in a quantum state of low vibration and low rotation. On the other hand, the linear configuration of HMgH in the ground state has been identified using the matrix isolation technique at 12 K to be the only stable structure after vibrational deactivation [2]. Thus the linear intermediate is expected to be long-lived. Then the resulting MgH may be energetically in a cold rotational and cold vibrational state. However, the decomposition of a bent structure through a linear geometry may possibly lead to rotational and vibrational excitation. Therefore, further study on the potential energy near the surface crossing and the lifetime of the linear intermediate will be conducive to a deep understanding of this reaction pathway. By analogy to our case, the rotational population of OH produced in the reaction of $O(^1D_2)$ atom with hydrocarbons RCH_2H (R = alkyl group) yields a bimodal distribution [12]. The minor component is rotationally and vibrationally cold. A mechanism causing an O insertion into CH bond to form a long-lived intermediate is expected. Before decomposition of RCH_2OH, its internal energy is randomized into various modes, so that the resulting OH becomes vibrationally and rotationally cold [12].

In the case of $Hg(6^3P_1)+H_2$ reaction [13–15] analogous to the Mg^*+H_2 reaction, the resulting HgH also forms a rotational bimodal distribution. Its mechanism, however, differs from our case. Because the Hg atom is heavy, a large spin-orbital coupling causes the dynamical behavior of the HgH product to be explained with Hund's case (c) [15]. Its low-N distribution results from an "indirect" reaction by tunneling through a low-energy barrier in a collinear geometric approach [13,15]. In contrast, the high-N distribution is caused by a "direct" reaction, in which the reaction coordinate along the $^3B_2$ surface (or $^3A'$) of the bent structure crosses the $^1A_1$ (or $^1A'$) surface of the ground state in a C_{2v} (or C_s) geometric approach. The H atom departs from the bent intermediate either through the excited $^3A'$ state or through the ground $^1A'$ state.

IV. CONCLUSION

With the measurement of rotational and vibrational population distribution of MgH($v''=0$ and 1) produced in the reaction of $Mg^*(^1P_1)$ with H_2, the mechanistic processes leading to the rotational bimodality can be clearly interpreted. The spectral analysis of MgH suggests that two mechanisms should be involved simultaneously to explain the reaction pathways for the removal of H atom from an intermediate MgH_2 along the exit-channel coordinate. One mechanism causes the resulting MgH populated in the low rotational levels and preferentially $v''=0$, and the other mechanism produces MgH in higher rotational levels with comparable $v''=0$ and $v''=1$ populations. For the major reaction pathway, the H atom is expected to escape from a bent configuration MgH_2, in which the bending mode activated initially may couple with the asymmetric stretch mode. The energy transfer into the asymmetric stretch mode causes an effective vibrational motion of the remaining MgH upon decomposition of MgH_2. In addition, a torque is exerted upon the MgH to cause population in the high rotational states. For the minor reaction pathway, the H atom is expected to escape from a linear intermediate HMgH. In this manner, the rotational torque is eliminated and the kinematic effect acts insignificantly upon the remaining MgH, such that the MgH product stays in a quantum state of low vibration and low rotation. Since the linear structure HMgH is long lived, its excess energy may have possibly randomized internally before decomposition. The resulting MgH may also be energetically in a cold vibrational and cold rotational state.

ACKNOWLEDGMENTS

The authors wish to thank Professor W. H. Breckenridge for critical reading of the manuscript and for providing very useful suggestions and discussion. This work is supported by the National Science Council of the Republic of China under Contract No. NSC82-0115-M001-170.

[1] W. H. Breckenridge and H. Umemoto, J. Chem. Phys. **80**, 4168 (1984).
[2] J. G. McCaffery, J. M. Parnis, G. A. Ozin, and W. H. Breckenridge, J. Chem. Phys. **82**, 4945 (1985).
[3] W. H. Breckenridge and J. H. Wang, Chem. Phys. Lett. **137**, 195 (1987).
[4] K. C. Lin and C. T. Huang, J. Chem. Phys. **91**, 5387 (1989).
[5] P. Chaquin, A. Sevin, and H. Yu, J. Phys. Chem. **89**, 2813 (1985).
[6] K. C. Lin and H. C. Chang, J. Chem. Phys. **90**, 6151 (1989).
[7] P. D. Kleiber, A. M. Lyyra, K. M. Sando, S. V. Zafiropulos, and W. C. Stwalley, J. Chem. Phys. **85**, 5493 (1986).
[8] G. Herzberg, *Molecular Spectra and Molecular Structure I: Spectra of Diatomic Molecules,* 2nd ed. (Van Nostrand Reinhold, New York, 1950), Chap. 5.
[9] L. T. Earls, Phys. Rev. **48**, 423 (1935).
[10] W. H. Breckenridge (private communication).
[11] R. D. Levine and R. B. Bernstein, *Molecular Reaction Dynamics and Chemical Reactivity,* (Oxford University Press, New York, 1987), Chap. 5.
[12] C. R. Park and J. R. Wiesenfeld, J. Chem. Phys. **95**, 8166 (1991), and the references therein.
[13] W. H. Breckenridge, C. Jouvet, and B. Soep, J. Chem. Phys. **84**, 1443 (1986).
[14] N. Bras, J. C. Jeannet, and D. Perrin, J. Chem. Phys. **87**, 219 (1987).
[15] A. Bernier and P. Millie, J. Chem. Phys. **88**, 4843 (1988).